

## Video Article

# Conducting Multiple Imaging Modes with One Fluorescence Microscope

Seongjin Park<sup>1</sup>, Jiacheng Zhang<sup>2</sup>, Matthew A. Reyer<sup>2</sup>, Joanna Zareba<sup>1,3</sup>, Andrew A. Troy<sup>4</sup>, Jingyi Fei<sup>1,2</sup><sup>1</sup>Department of Biochemistry and Molecular Biology, University of Chicago<sup>2</sup>The Institute for Biophysical Dynamics, University of Chicago<sup>3</sup>Faculty of Chemistry, Wrocław University of Science and Technology<sup>4</sup>Nikon Instruments Inc.Correspondence to: Jingyi Fei at [jingyifei@uchicago.edu](mailto:jingyifei@uchicago.edu)URL: <https://www.jove.com/video/58320>DOI: [doi:10.3791/58320](https://doi.org/10.3791/58320)

Keywords: Bioengineering, Issue 140, Fluorescence microscopy, super-resolution imaging, smFRET, STORM, PALM, TIRF

Date Published: 10/28/2018

Citation: Park, S., Zhang, J., Reyer, M.A., Zareba, J., Troy, A.A., Fei, J. Conducting Multiple Imaging Modes with One Fluorescence Microscope. *J. Vis. Exp.* (140), e58320, doi:10.3791/58320 (2018).

## Abstract

Fluorescence microscopy is a powerful tool to detect biological molecules *in situ* and monitor their dynamics and interactions in real-time. In addition to conventional epi-fluorescence microscopy, various imaging techniques have been developed to achieve specific experimental goals. Some of the widely used techniques include single-molecule fluorescence resonance energy transfer (smFRET), which can report conformational changes and molecular interactions with angstrom resolution, and single-molecule detection-based super-resolution (SR) imaging, which can enhance the spatial resolution approximately ten to twentyfold compared to diffraction-limited microscopy. Here we present a customer-designed integrated system, which merges multiple imaging methods in one microscope, including conventional epi-fluorescent imaging, single-molecule detection-based SR imaging, and multi-color single-molecule detection, including smFRET imaging. Different imaging methods can be achieved easily and reproducibly by switching optical elements. This set-up is easy to adopt by any research laboratory in biological sciences with a need for routine and diverse imaging experiments at a reduced cost and space relative to building separate microscopes for individual purposes.

## Video Link

The video component of this article can be found at <https://www.jove.com/video/58320/>

## Introduction

Fluorescence microscopes are important tools for the modern biological science research and fluorescent imaging is routinely performed in many biology laboratories. By tagging biomolecules of interest with fluorophores, we can directly visualize them under the microscope and record the time-dependent changes in localization, conformation, interaction, and assembly state *in vivo* or *in vitro*. Conventional fluorescence microscopes have a diffraction-limited spatial resolution, which is ~200 - 300 nm in the lateral direction and ~500 - 700 nm in the axial direction<sup>1,2</sup>, and are, therefore, limited to imaging at the 100s of nanometers-to-micron scale. In order to reveal finer details in the molecular assembly or organization, various SR microscopies that can break the diffraction limit have been developed. Strategies used to achieve SR include non-linear optical effects, such as stimulated emission depletion (STED) microscopy<sup>3,4</sup> and structured illumination microscopy (SIM)<sup>5,6,7</sup>, stochastic detection of single molecules, such as stochastic optical reconstruction microscopy (STORM)<sup>8</sup> and photoactivated localization microscopy (PALM)<sup>9</sup>, and a combination of both, such as MINFLUX<sup>10</sup>. Among these SR microscopies, single-molecule detection-based SR microscopes can be relatively easily modified from a single-molecule microscope set-up. With repetitive activation and imaging of photoactivatable fluorescent proteins (FPs) or photo-switchable dyes tagged on biomolecules of interest, spatial resolution can reach 10 - 20 nm<sup>11</sup>. To gain information on molecular interactions and conformational dynamics in real-time, angstrom-to-nanometer resolution is required. smFRET<sup>12,13</sup> is one approach to achieve this resolution. Generally, depending on the biological questions of interest, imaging methods with different spatial resolutions are needed.

Typically, for each type of imaging, specific excitation and/or emission optical configuration is needed. For instance, one of the most commonly used illumination methods for single-molecule detection is through total internal reflection (TIR), in which a specific excitation angle needs to be achieved either through a prism or through the objective lens. For smFRET detection, emissions from both donor and acceptor dyes need to be spatially separated and directed to different parts of the electron-multiplying, charge-coupled device (EMCCD), which can be achieved with a set of mirrors and dichroic beam splitters placed in the emission path. For three-dimensional (3-D) SR imaging, an optical component, such as a cylindrical lens<sup>14</sup>, is needed to cause an astigmatism effect in the emission path. Therefore, homebuilt or commercially available integrated microscopes are, usually, functionally specialized for each type of imaging method and are not flexible to switch between different imaging methods on the same set-up. Here we present a cost-effective, hybrid system that provides adjustable and reproducible switches between three different imaging methods: conventional epi-fluorescent imaging with diffraction-limited resolution, single-molecule detection-based SR imaging, and multi-color single-molecule detection, including smFRET imaging (**Figure 1A**). Specifically, the set-up presented here contains fiber-coupled input lasers for multi-color excitation and a commercial illumination arm in the excitation path, which allows programmed control of the excitation angle, to switch between epi-mode and TIR mode. In the emission path, a removable homebuilt cylindrical lens cassette is placed within the

microscope body for 3-D SR imaging, and a commercial beam splitter is placed before an EMCCD camera that can be selectively enabled to detect multiple emission channels simultaneously.

## Protocol

### 1. Microscope Design and Assembly

#### 1. Excitation path

NOTE: The excitation path includes lasers, differential interference contrast (DIC) components, the microscope body, and its illumination arm.

1. Prepare a vibration-isolated optical table. For example, a structural damping table of 48 x 96 x 12" gives enough space for all the components.  
NOTE: Build the set-up in a room with temperature control (e.g., 21.4 ± 0.55 °C). Temperature stability is critical to maintaining the optical alignment.
2. Install a microscope body that is equipped with an illumination arm for optical fiber connection, a 100X oil-immersion TIRF objective lens, and DIC components.
3. Place four laser heads (647 nm, 561 nm, 488 nm, and 405 nm, encircled in **Figure 1B**) and their heat sinks on the optical table, and make sure the emitted laser beams have the same height and are as short as possible to ensure good stability (e.g., 3").  
NOTE: If a laser head sits at a shorter height than other lasers, put an aluminum plate with adequate thickness underneath it. Always ensure maximum contact between the heat sinks and the optical table for the best heat dissipation (**Figure 1B**). The lasers need to be powerful enough for SR imaging. See **Table of Materials**. It is recommended to have laser clean-up filters in front of diode lasers.
4. Install a data acquisition card through a peripheral component interconnect (PCI) interface in a workstation and connect lasers with this card. Control the lasers' ON/OFF behaviors by transistor-transistor logic (TTL) output, and their power adjustment by the analog output of this card (**Figure 1C**). Install a proper microscopy imaging software (either commercial or homebuilt) to control the data acquisition card, as well as the microscope body.
5. Mount the mirrors and dichroic beam splitters (590, 525, and 470 long pass filters) to their respective mounts. Use very stable mirror mounts for the mirrors. Use circular splitters with retaining rings to avoid any bending of the dichroic beam splitters (**Figure 1D**).
6. Place the mirrors and dichroic beam splitters on the optical table to combine the laser beams (**Figure 1B**). To achieve the most stable alignment, make the whole arrangement as compact as possible, and use 1"-thickness optical posts. Arrange the lasers so that the shorter wavelength lasers are closer to the optical fiber coupling (**Figure 1B**) since short-wavelength lights dissipate more in the air.
7. Combine laser beams into a single-mode optical fiber. To do so, build a fiber coupler in a cage system through the following steps:
  1. Mount a fiber adapter plate in a z-axis translation mount (**Figure 1E**, leftmost panel).
  2. Mount an achromatic doublet lens (focal length = 7.5 mm) in a cage plate (**Figure 1E**, second panel from the left).
  3. Connect the two parts above by extension rods to form a cage. Mount the cage on the optical table with mounting brackets on the 1"-thick optical posts (**Figure 1E**, middle panel).
  4. Align the 647-nm laser first with a single-mode optical fiber (FC/APC end to the coupler).  
NOTE: A rough alignment using a multi-mode optical fiber before using the single-mode optical fiber may help the alignment process. Adjust the angles of the mirrors and dichroic beam splitters (**Figure 1D**, by adjustment knobs), as well as the distance between the achromatic doublet lens and the fiber adapter plate (**Figure 1E**, by adjusting z-axis translation mount) to gain maximum laser power output through the fiber.
  5. Once the alignment of the first laser is done, temporarily install a pair of irises and align the rest of the lasers one by one (**Figure 1F**). Check the alignment efficiency with a power meter.
  6. Leave one iris in the front of the adapter plate to reduce the reflections of the lasers.  
NOTE: Strong back reflections can reduce the lifetime of laser sources. Optionally, an optical isolator can be installed in front of each laser head to remove the reflections completely.
8. Connect the other end of the optical fiber to the illumination arm of the microscope (**Figure 1H**).
9. Design and install the "magnification lens (mag lens)" through the following steps:  
NOTE: The lasers can be used for epi-fluorescence imaging of the sample, but the narrow beam size of each laser limits the illuminated area of the sample to an area several times smaller than the actual size of the corresponding camera sensor, especially for the newer cameras (with 18.8 mm in diagonal length compared to the conventional 11.6-mm length). Thus, it is desirable to expand the beam to achieve a larger and flatter illumination of the sample.
  1. Design the mag lens, which can fit into the illumination arm (**Figure 1H**).  
NOTE: The design of the mag lens depends on where it will be installed. **Figure 1H** shows an example of the installation in the illumination arm, but it can be installed in any spot after the laser beams are collimated (see **Discussion**). Design it with a computer-aided design and drafting software.
  2. Place two achromatic lenses, one concave (focal length =  $f_1$ ), and one convex (focal length =  $f_2$ ) in the home-made mag lens holder (**Figure 2A** and **2C**), with the distance equal to the sum of their focal lengths,  $f_1 + f_2 = (-25) + 50 = 25$  mm (**Figure 2B**).  
NOTE: With this choice of focal lengths, the mag lens expands the beam by  $f_2/|f_1| = 2$  folds. The mag lens provides versatility. It can be removed to resume regular illumination without expanding the beams (**Figure 2D**) or inserted in the reverse direction to focus the laser beam to achieve a stronger excitation intensity.

### 2. Emission path

NOTE: The emission path is composed of a removable cylindrical lens, a barrier filter wheel, an emission splitter, and an EMCCD camera (**Figure 1G**). To attain the best point spread function (PSF) of single molecules, the DIC prism is put away from the objective lens.

1. Custom-design the cylindrical lens (3-D lens) cassette, which can fit into the manual DIC analyzer insert slot in the microscope body (**Figure 3C**).  
NOTE: This design does not compromise the DIC analyzer since an analyzer block can be inserted in the filter turret.
2. Place the 3-D lens of 10 m of focal length in the cassette and insert it into the emission beam path to create the astigmatism effect necessary for extracting the z coordinate of every single molecule<sup>14</sup>.  
NOTE: Optionally, the 3-D lens cassette can be placed in or out of the emission path (**Figure 3C**).
3. Install a multi-band dichroic beam splitter in the filter turret inside of the microscope body.
4. Install emission filters.  
NOTE: The emission filters are chosen depending on the preferred fluorophores. Depending on the imaging module, emission filters placed in different locations are used as described below:
  1. For sequential multi-color epi-fluorescence imaging or SR imaging, use emission filters placed in the barrier filter wheel connected next to the microscope body to minimize the vibration in the microscope body during channel switch (**Figure 1G**).
  2. For simultaneous multi-color detection (e.g., smFRET experiments), place another filter set in an emission splitter (check step 4 for details).  
NOTE: Usually, a commercial emission splitter has two switchable modes (i.e., “engaged” or “bypass” modes). To separate emission lights chromatically for simultaneous multi-color imaging (“engaged” mode), a filter cube holding two dichroic beam splitters and three emission filters is used (“triple cube,” **Figure 4C and 4D**). An empty slot in the barrier filter wheel is used in combination with the triple cube. On the other hand, for sequential multi-color imaging, the triple cube is replaced by a cube that just has a mirror inside (“bypass cube,” **Figure 4A and 4D**).
5. Install the EMCCD camera as the last part of the emission path. Utilize the USB-PCI connection to achieve a fast frame rate.  
NOTE: An EMCCD camera is recommended for the most sensitive single-molecule detection, but an advanced sCMOS camera can be an alternative.

### 3. Diffraction-limited Imaging with Epi-excitation

1. Adjust the excitation lasers' incidental angle to epi-mode in the illumination arm.
2. Disengage the 3-D lens if engaged (**Figure 3C**, right panel).
3. Insert the bypass cube in the emission splitter (**Figure 4A and 4E**, bottom panel).
4. (Optional) Insert the mag lens for a broadened illumination area (**Figure 2D**, left panel).  
NOTE: With the use of a mag lens and a 100X oil-immersion objective lens, about  $91 \times 91 \mu\text{m}^2$  can be illuminated evenly, eliminating the need to use a white light source and multiple filter cubes.
5. Use a microscopy imaging software to take multi-channel, and/or Z-stack, and/or time-lapse images.  
NOTE: There are multiple programs available for microscopy imaging, not only from microscope manufacturers but also from third-party companies or open source developers.

### 4. Multi-channel Single-molecule Imaging Including smFRET

NOTE: Move to an “empty” position in the barrier filter wheel, so that all the emission with any wavelength can reach to the second set of filters/dichroic beam splitters in the emission splitter.

1. To set up multi-color single-molecule detection of surface-immobilized molecules<sup>15</sup> using TIRF excitation, including smFRET measurement, adjust the excitation lasers' incidental angle to the TIRF angle. Disengage the mag lens and the 3-D lens.
2. Engage the three-channel mode in the emission splitter (**Figure 1G**) through the following steps:
  1. Replace the bypass cube with a “calibration cube” that allows light to go through all channels (**Figure 4B and 4E**).
  2. Turn on the camera under DIC (i.e., no emission filter in the barrier filter wheel) and adjust the aperture of the emission splitter until three fully separated channels appear on the screen.  
NOTE: Conduct this step with the room light lit, to visualize all the channels.
  3. Turn the vertical/horizontal adjustment control knobs on the emission splitter and roughly align the three channels (**Figure 4E and 4F**).
  4. Turn off the camera and replace the calibration cube with a triple cube (**Figure 4C and 4E**).
  5. Place a sample with 100-nm multichannel beads on top of the 100X objective lens and focus on the sample.
  6. Turn on the camera and the 488-nm laser, zoom in on one of the bright beads, and finely align the three channels by turning the adjustment control knobs again (**Figure 4E and 4G**).  
NOTE: 100-nm multichannel beads emit different wavelengths of light upon 488-nm excitation, enabling the three-channel alignment.
3. Turn on the camera and lasers, focus, and find a good position with a reasonable spot density. Adjust the laser power and exposure time to achieve acceptable signal-to-noise and photobleaching levels. Use the microscopy imaging software to take time-lapse images.

### 5. SR Imaging

NOTE: This is single-molecule detection-based SR microscopy.

1. To set up SR imaging, insert the 3-D lens and remove the mag lens. Set the exposure time of the camera in the appropriate laser channels (e.g., 5 - 60 ms). Determine and manually set the optimal excitation lasers' incidental angle to be the TIRF angle.
2. Place the sample in SR imaging buffer<sup>16</sup>. Allow the buffer to equilibrate for at least 10 min before imaging.  
NOTE: SR imaging buffer expires after roughly 1 h, so make new SR imaging buffer accordingly.
3. Take a DIC image before SR imaging. In order to find the proper objective height for SR, which optimizes the astigmatism effect, use DIC imaging to find the middle plane of the cells. Identify the plane by the height at which the cells transition from “light” to “dark” images and

- appear to become transparent (**Figure 5A, 5B, and 5C**). Once the desired focal plane is determined, engage the z-drift correction system (**Figure 1A**).
- Conduct SR imaging. Change the 405-nm laser power to maintain a reasonable density of 'blinking-on' spots.  
NOTE: While it is possible to change the 405-nm laser manually, it is more convenient to run a programmed data acquisition code to maintain the density of "blinking-on" spots. Here is an example of how it is conducted automatically. The source code is available upon request (**Figure 6**).
    - Start the imaging acquisition with 0 W/cm<sup>2</sup> violet laser power.
    - Count the number of blinking-on spots in a certain period.
    - Modulate the violet laser power so that the number of blinking-on spots is kept above a user-defined "counting threshold" in the field of view. Increase the violet laser power when the number of blinking-on spots drops below the counting threshold.
    - Terminate the acquisition when the number of blinking-on spots drops below the counting threshold using the maximum violet laser power.  
NOTE: The maximum can be set differently depending on the sample brightness, but no higher than 130 W/cm<sup>2</sup>. Depending on the actual goal of the SR imaging, this automatic acquisition code can be manually terminated at any desired point.
  - Check the blinking behavior and PSFs of the spots soon after beginning the acquisition.  
NOTE: If the blinking behavior is not ideal, change the excitation lasers' incidental angle or replace the imaging buffer. Expect a sampling of "vertical", "horizontal", and "diamond" shapes of PSF, representing fluorophores from below, above, and within the focal plane, respectively (**Figure 5D**). If most spots show either vertical or horizontal PSFs, then the focal plane is off from the center of the cells, so terminate the experiment and adjust the focal plane again. A presence of air bubble in the immersion oil or other local factors can affect the PSFs' quality, so it may be necessary to replace the oil or change to a different imaging area of the sample.
  - For the data analysis, use either open source (in NIH ImageJ plugins) or commercially available codes to detect centroids of each spot in each imaging frame and extract z-values of each spot from x- and y-widths<sup>14</sup>.  
NOTE: In this report, a source code originally developed in one of the earliest single-molecule detection-based SR<sup>8</sup> was modified for 3-D detection<sup>16</sup> and was used.
  - In the case of two-color imaging, image the fluorophore with the longer excitation wavelength, followed by the one with the shorter excitation wavelength. Run the automated acquisition code similarly to the one described in step 5.4, but with a different imaging laser.  
NOTE: Chromatic aberration should be corrected between images with different fluorophores (e.g., red dye and yellow-green dye). Here are the steps.
    - Immobilize multiple 100-nm multichannel beads on the glass coverslip, avoiding forming clusters.
    - Take images of them in different excitation channels.
    - Extract their (X, Y, Z) coordinates by software (step 5.6).
    - Plot  $\Delta X_i = X_{1i} - X_{2i}$  and  $\Delta Y_i = Y_{1i} - Y_{2i}$  (i is for different beads, and 1 and 2 are different color channels) separately and fit them with proper functions. Save the functions.  
NOTE: Linear functions are sufficient in most cases. Once these functions are determined, this measurement does not have to be repeated each time of imaging.
    - In the actual two-color SR imaging of a sample of interest, apply the functions to correct (X, Y) chromatic aberration. For z-directional chromatic aberration, conduct it by obtaining  $\Delta Z = Z_1 - Z_2$  for multichannel beads or known reference multichannel samples seeded together with the sample of interest.  
NOTE: Unlike (X, Y) chromatic aberration, z-directional chromatic aberration is not well-reproducible in each experiment, mainly due to incomplete z-directional focus maintenance upon channel switching. Thus, it is recommended to conduct the correction each time.  $\Delta Z = Z_1 - Z_2$  is mostly independent of (X, Y), so just a few beads or reference samples would be sufficient per each sample area of interest. Plot the constructed final two-color SR images in a 3-D visualization software and check  $\Delta Z$  manually.

## Representative Results

This microscope allows flexible and reproducible switching between different imaging methods. Here we show sample images collected with each imaging module.

**Figure 5D** demonstrates the PSF of the blinking-on molecule during the SR acquisition. Thousands of such images are reconstructed to generate the final SR image (**Figure 5E**). **Figure 5E** shows the same bacterial regulatory RNAs as shown in the epi-fluorescence image in **Figure 7A**. **Figure 7** shows the representative epi-fluorescence images of a small regulatory RNA in *Escherichia coli* cells and an mRNA in U2OS mammalian cells. Both RNAs are labeled with fluorophore-tagged DNA oligo through *in situ* hybridization<sup>17</sup>. **Figure 8** shows the representative smFRET measurement of folded RNA molecules labeled with donor dye (green dye) and acceptor dye (red dye). The complexes are immobilized on the microscope slide, and excited by TIRF illumination. Fluorescence intensity trajectories can be extracted from individual single molecules, generating FRET efficiency as a function of time.

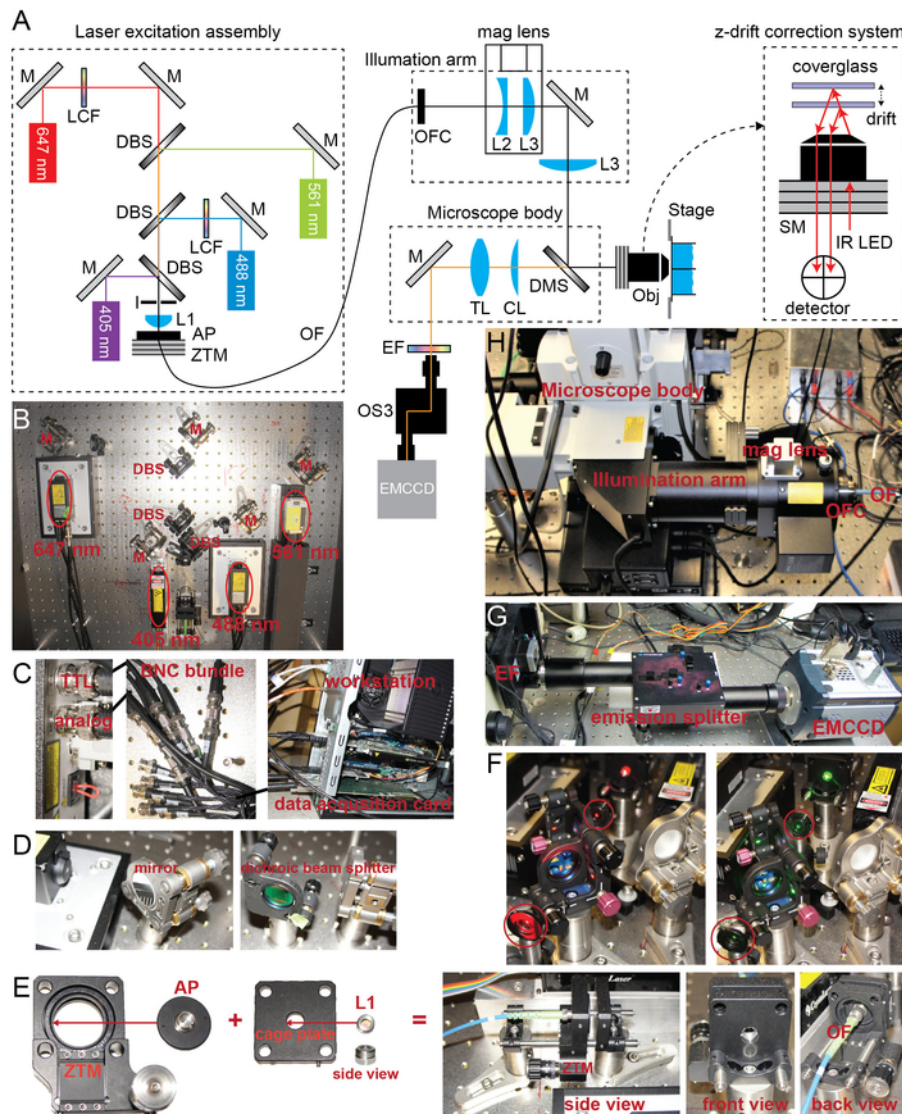


**Figure 1: The design of the microscope set-up.** (A) This panel shows a diagram of the set-up. M = mirror, DBS = dichroic beam splitter, LCF = laser clean-up filter, I = iris, L = lens, AP = adapter plate, ZTM = z-axis translational mount, OF = optical fiber, OFC = optical fiber coupling, CL = cylindrical lens, TL = tube lens, EF = emission filter(s), Obj = objective lens, and SM = step motor. The z-drift correction system moves the step motor on the nosepiece of the objective lens to the opposite direction of the z-drift, which is calculated by the infrared (IR) signal generated by its own LED and detected by its own detector. (B) This panel shows the laser excitation assembly. Four lasers are combined through mirrors and dichroic beam splitters and are then directed to an optical fiber through a focusing lens and an adapter plate sitting on a translational mount (bottom of the picture). (C) This panel shows the laser modulation. Two Bayonet Neill-Concelman (BNC) cables are connected to each of the laser (either the head or the controller, depending on the manufacturer) for TTL and analog modulation (leftmost panel). BNC cables are combined into a single cable (middle panel) which is connected to a data acquisition card in a workstation (rightmost panel) for computer control. (D) This panel shows the mirror and dichroic beam splitter mounts. (E) Building a fiber coupler in a cage system. A fiber adapter plate (AP) is mounted in a z-axis translation mount (ZTM) so that its distance to the achromatic double lens (L1, side view shown) can be modulated. AP and ZTM have matching threads, same as L1 and the cage plate. (F) A pair of irises (encircles) are installed during the alignment procedure for multiple lasers. They are used to ensure that the 647-nm laser (left panel) and the 561-nm laser (right panel) go through the same path. (G) A partial portion of the emission path is shown. Outside of the microscope body, the emission filter wheel, the emission splitter, and the EMCCD camera are installed in order. (H) This panel shows the illumination arm assembly. The mag lens is inserted into the illumination arm. The excitation laser beams are sent to the illumination arm through the optical fiber and the optical fiber coupling (at the right-hand side of the picture). [Please click here to view a larger version of this figure.](#)

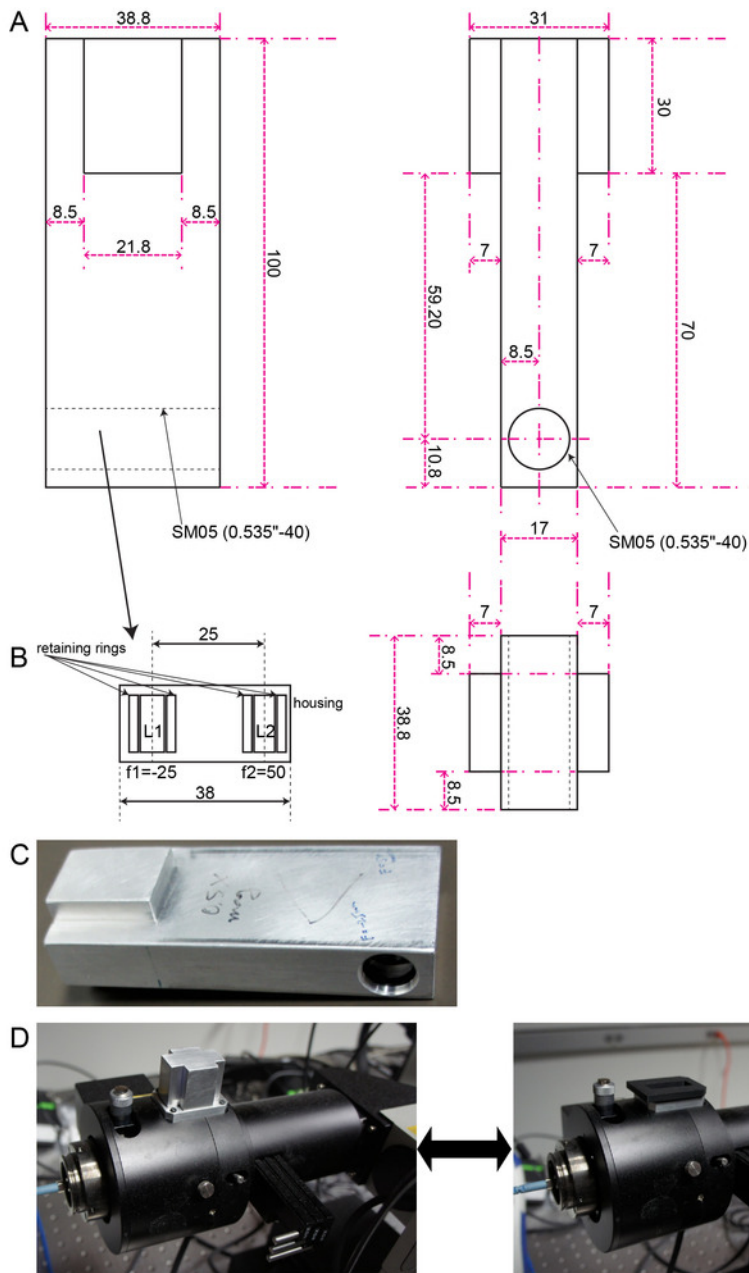


**Figure 2: The mag lens.** (A) This panel shows orthographic projections of the holder housing lenses for magnifying laser beams (unit: mm). This design is intended to fit into the illumination arm. (B) This panel shows an internal drawing of the hole in the holder where two lenses get in. L1 is a concave lens and L2 is a convex lens, and the distance between them is the sum of their focal lengths. (C) This is a photo of the mag lens. (D) The mag lens can be inserted in the illumination arm to expand or focus the laser beams (left) or can be removed to keep the laser beams unchanged (right). [Please click here to view a larger version of this figure.](#)

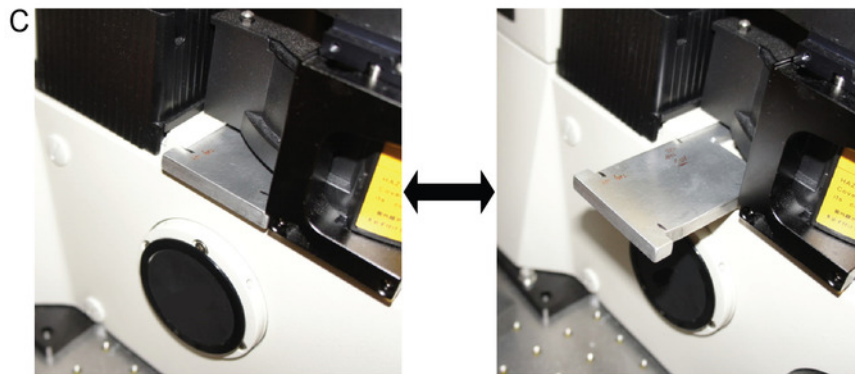
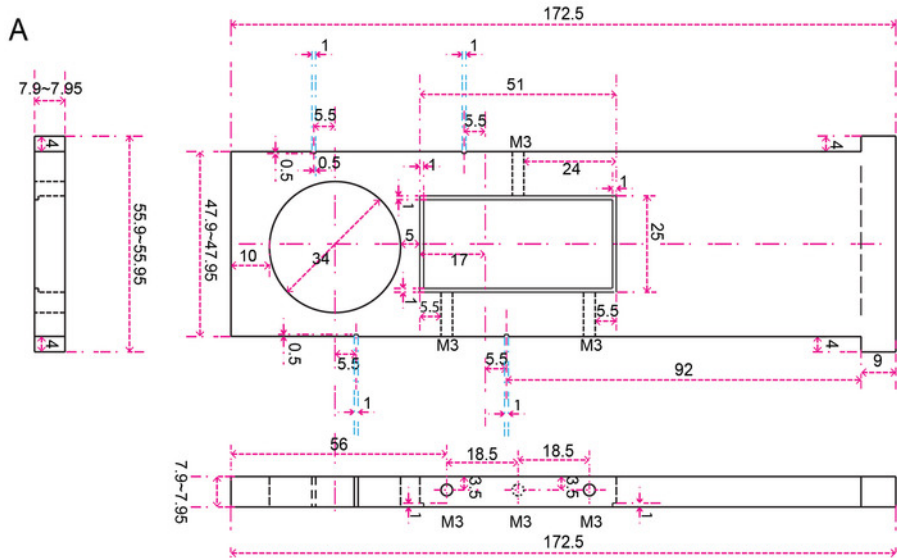


**Figure 3: The 3-D lens.** (A) This panel shows orthographic projections of the holder having a blank circular hole for the bypass mode and a rectangular hole for holding the cylindrical lens (unit: mm). This design is intended to be fit to the DIC analyzer slider in a microscope body. (B) This is a photo of the 3-D lens. (C) The cylindrical lens can be engaged in the emission beam path to cause PSFs with astigmatism (left) or can be disengaged for the bypass mode, keeping the PSFs intact (right). [Please click here to view a larger version of this figure.](#)

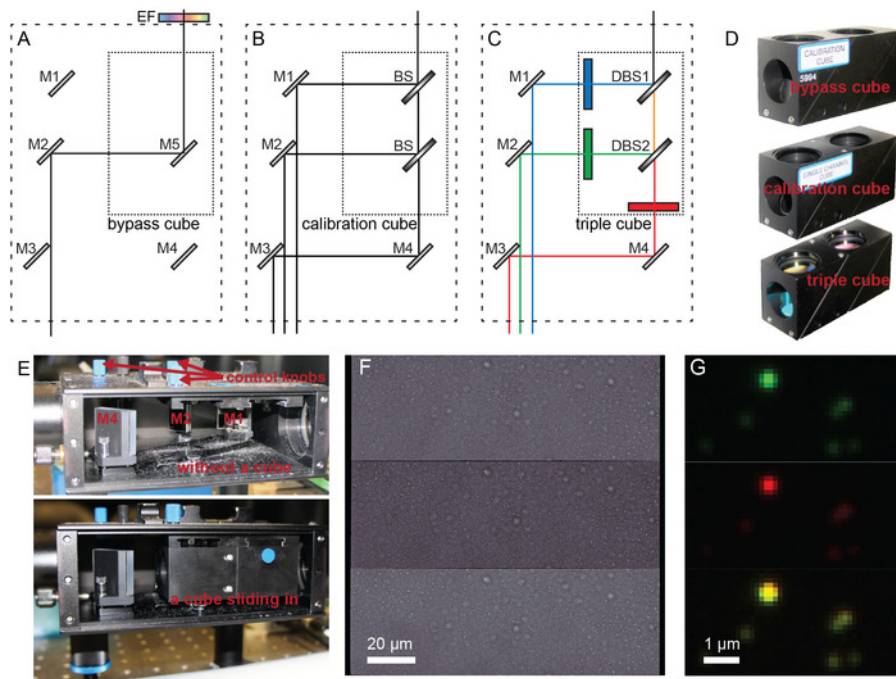


**Figure 4: Multi-channel alignment of the emission splitter.** Schemes of optics and light path are shown in the emission splitter with (A) a bypass cube, (B) a calibration cube, and (C) a triple cube. M = mirror. The bypass cube has a mirror inside (M5) and is supposed to be used with an emission filter (EF) in the barrier filter wheel. The calibration cube has beam splitters (BS) that allow lights to go through all channels. The triple cube has two dichroic beam splitters (DBS), as well as three emission filters. (D) These are photos of the three cubes. (E) The internal of the emission splitter is shown without a cube (upper panel) and with a cube (lower panel) sliding in. Control knobs for the mirrors are on top of the emission splitter (upper panel). M3 is behind M4 and not captured in the photo. (F) This panel shows channel alignment using the calibration cube under DIC. (G) This panel shows a fine alignment of the green (top panel) and red (middle panel) channels using 100-nm multichannel beads and a triple cube. A merged image of the two channels is also shown (bottom panel). [Please click here to view a larger version of this figure.](#)

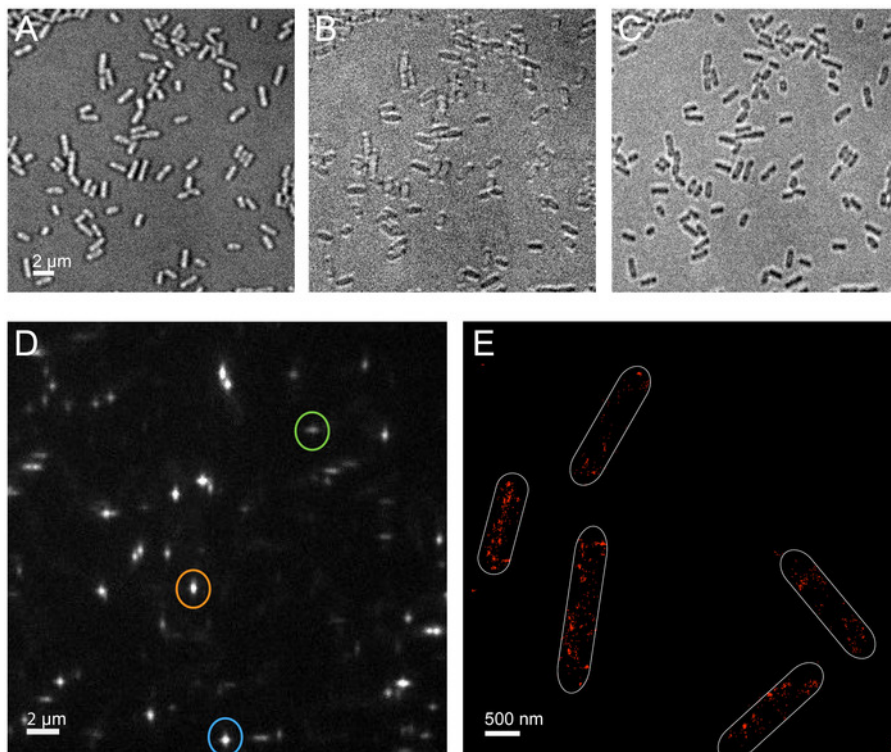


**Figure 5: Representative SR image acquisition.** These panels show a representative DIC image (A) below, (B) at, or (C) above the central plane of the cells. (D) This panel shows an example of the PSF of the blinking-on fluorophores. The orange circle surrounds a "vertical" PSF. The green circle surrounds a "horizontal" PSF. The blue circle surrounds a diamond-shaped PSF, representing fluorophores at a focused plane. (E) This panel shows a representative reconstructed SR image. A small regulatory RNA is labeled with fluorescence *in situ* hybridization with red dye. The white borders mark the edges of the cells. [Please click here to view a larger version of this figure.](#)

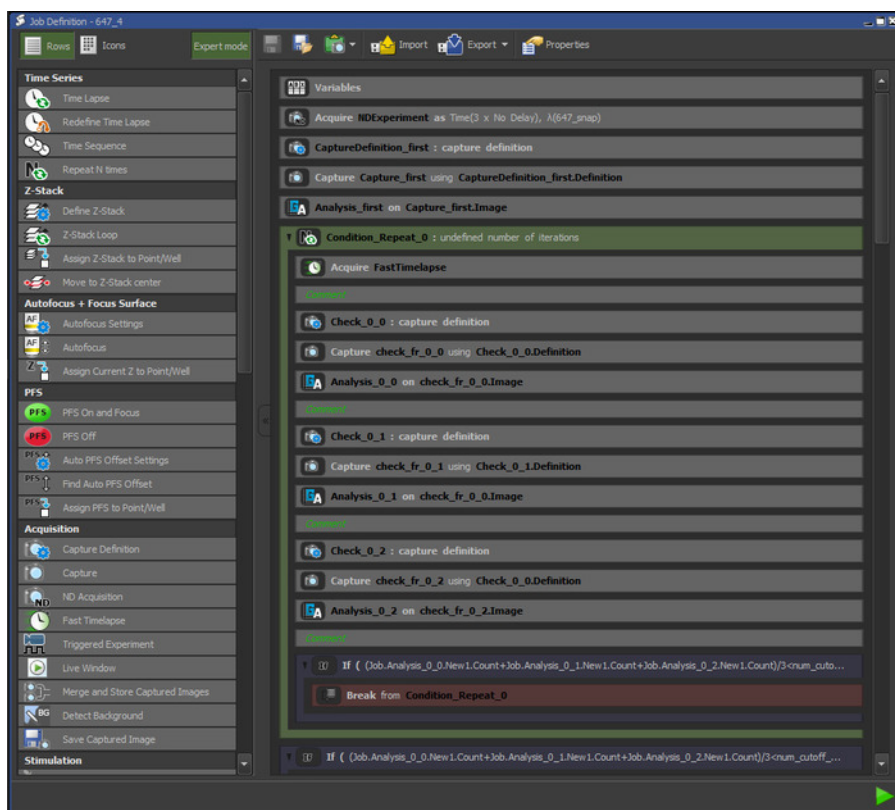


**Figure 6: A programmed data acquisition code for SR imaging.** In this programmable acquisition module, various execution commands and microscope control functions are listed in the left panel and can be selected to create programmed acquisition code. The commands are executed sequentially from top to bottom. This screenshot shows an example where a predefined certain number of iterated imaging acquisitions are conducted until the acquisition is posed and the number of spots in three sequential image frames is calculated. If the average number of these spots are above the threshold (defined as 50% of the number of cells in bacterial imaging), the image acquisition continues in the same loop. If below the threshold, then the image acquisition continues in the next loop where stronger violet laser power is used (cut at the bottom of the screenshot). [Please click here to view a larger version of this figure.](#)

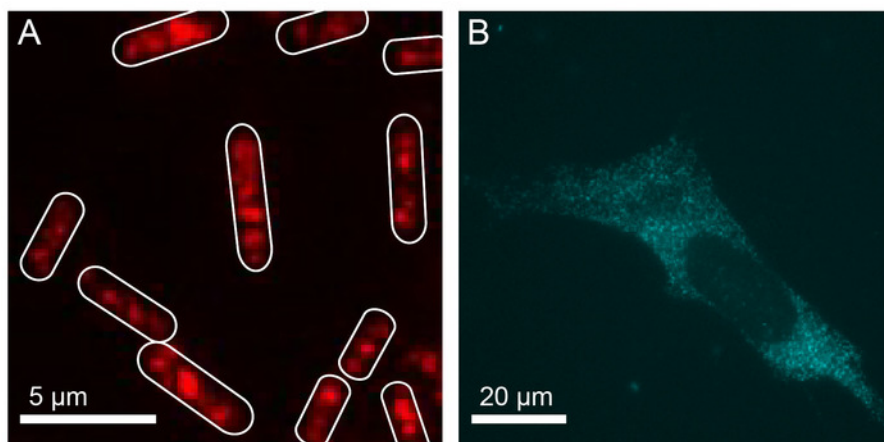


**Figure 7: Representative epi-fluorescence images.** (A) This panel shows a small regulatory RNA in *E. coli* cells. (B) This panel shows an mRNA in U2OS mammalian cells. RNAs are labeled with red dye and blue dye through fluorescence *in situ* hybridization. [Please click here to view a larger version of this figure.](#)

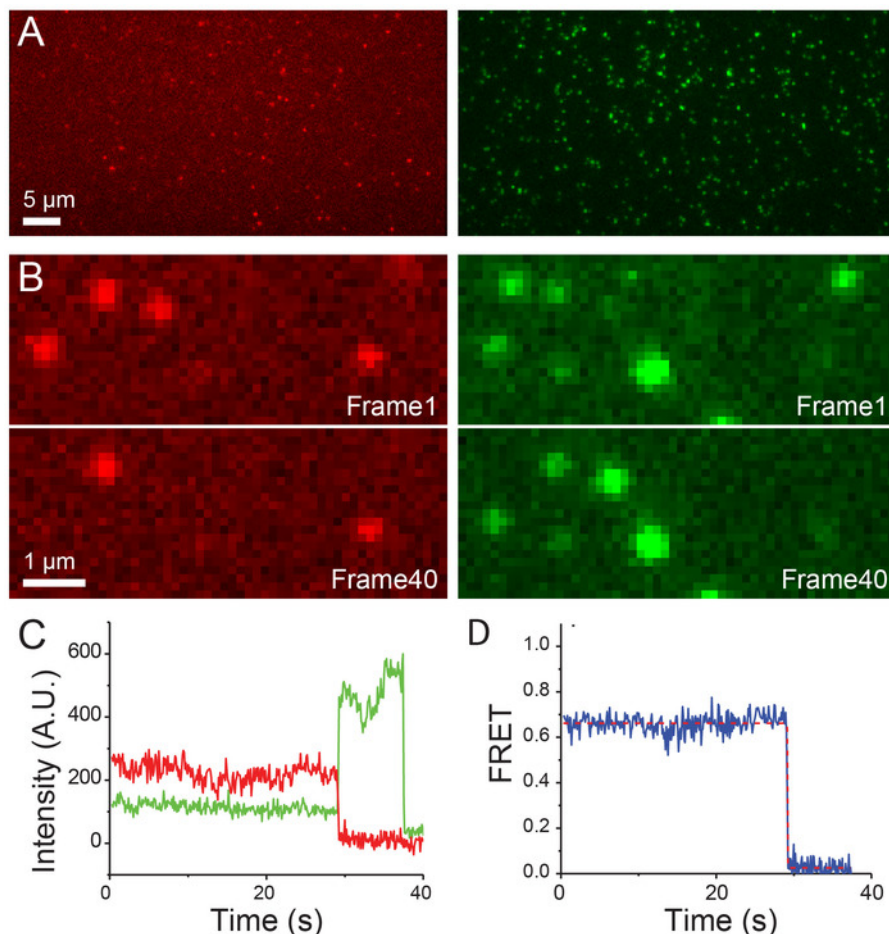


**Figure 8: Example of smFRET imaging.** (A) Samples were excited with the 561-nm laser. (B) Emissions from the green and red dyes are collected simultaneously and shown as green (right) and red (left) spots, respectively. (C) This panel shows the representative fluorescence intensity vs. time trajectories of green dye (green) and red dye (red) from one molecule. (D) This panel shows the FRET efficiency vs. the time trajectory (solid blue line) calculated as  $I_{\text{Acceptor}} / (I_{\text{Donor}} + I_{\text{Acceptor}})$  from one molecule of the sample. The FRET trace is fitted with the Hidden Markov Model (dashed red line). [Please click here to view a larger version of this figure.](#)

## Discussion

This hybrid microscope system eliminates the need to purchase multiple microscopes. The total cost for all parts, including the optical table, table installation labor, software, and workstation, is about \$230,000. Custom-machined parts, including the mag lens and 3-D lens, cost around \$700 (the cost depends on the actual charges at different institutes). Typical commercially available integrated systems for single-molecule detection-based SR microscopy cost more than \$300,000 ~ 400,000 and are not readily available for smFRET measurement, or epi-imaging for a reasonable field of view, without white light source. Thus, the approach presented here can achieve imaging capabilities equivalent to multiple microscopes at a significantly reduced cost.

This modulated microscope system can be based on microscope bodies from different manufacturers. The 3-D lens can potentially be installed in any position in the emission path, including inside the emission splitter, within the microscope body, or in available space between the filter wheel and the objective nosepiece. However, the physical location of the 3-D lens will determine its focal length for achieving the best astigmatism effect for 3-D SR imaging. We recommend starting with a 10-m focal length. The mag lens is essentially a beam expander installed in the excitation path. If the excitation lasers are air-coupled (*i.e.*, without optical fiber), it is trivial to install such an expander in any spot after the laser beams are collimated. If the excitation lasers are fiber-coupled, then look for extra slots to install two lenses (one concave and the other one convex). For example, many commercial illumination arms have slots for neutral-density filters. Find two lenses with the sum of their focal lengths equal to the distance between the two slots. Then, they can be inserted to function as a mag lens. Alternatively, a mount for the field diaphragm slider can be another place, if available. Building the mag lens in a removable cassette has the additional advantage of enabling one to focus the excitation lasers to achieve higher power, which may be necessary for SR imaging, simply by flipping the orientation of the mag lens.

In this report, we demonstrated flexible switching between three different imaging techniques using a modulated microscope. This set-up can be used for broader and more advanced applications. For example, the SR configuration can be used for single-particle tracking in live cells, on photo-switchable or photoactivatable fluorescent protein-tagged biomolecules of interest<sup>18,19</sup>. The smFRET configuration can be used to study molecular interactions in *in vivo* systems<sup>20</sup>. The emission splitter-based multi-channel detection can be combined with the SR configuration to perform two-color SR imaging or single-particle tracking simultaneously<sup>21</sup>.

This set-up can be further expanded to enable more modulated components. For example, another layer of filter turret and illumination compartment can be added, so that additional excitation/emission paths can be created for additional channels, such as one with an infrared (IR) laser for imaging samples labeled with IR dyes. In addition to allowing the added imaging channel, IR lasers can be used to correct the stage drift in SR imaging either during imaging acquisition or during the post analysis. For drift correction during imaging acquisition, if the z-drift correction system is not available from the microscope manufacturer, an alternative system with IR laser can be either homebuilt<sup>14</sup> or acquired from third-party companies. For post-acquisition drift correction, an IR laser can be used for tracking fiducial markers.<sup>22</sup>

Single-molecule detection-based SR microscopy requires two sets of software, one for data acquisition and one for data analysis. For data acquisition, even a simple homebuilt software that takes images through the camera while controlling the lasers' ON/OFF behaviors can work to generate SR images, while it is possible to manually modulate the 405-nm laser power, e.g., by rotating a gradient neutral-density filter installed in front of the laser. However, this way of conducting the experiment is dependent on the experimenter's subjective judgment of the density of blinking-on spots. Thus, this way is not objective and may not be suitable to be used for the quantification of SR imaging data. The data acquisition code used here includes spot detection/a counting algorithm while the data acquisition is ongoing, enabling automatic modulation of the 405-nm laser power based on the density of blinking-on spots (Figure 6). Nowadays, some microscope manufacturers provide programmable imaging modules, so one can utilize these, or look for plugins from open sources like Micro-Manager. For the data analysis, it is possible to use commercially available analysis modules from microscope manufacturers or look for plugins from open sources like ImageJ.

In summary, the set-up presented here provides high versatility and easy switching between different imaging configurations at a reduced cost and space. This set-up is relatively easy to adopt by any research laboratory in biological sciences with a need for routine and diverse imaging experiments.

## Disclosures

The authors have nothing to disclose.

## Acknowledgements

J.F. acknowledges support from the Searle Scholars Program and the NIH Director's New Innovator Award. The authors acknowledge useful suggestions from Paul Selvin's lab (University of Illinois, Urbana-Champaign) for positioning the 3-D lens.

## References

- Lipson, S. G., Lipson, H., Tannhauser, D. S. *Optical physics*. Cambridge University Press. Cambridge, UK; New York, NY (1995).
- Török, P., Wilson, T. Rigorous theory for axial resolution in confocal microscopes. *Optics Communications*. **137** (1-3), 127-135 (1997).
- Klar, T. A., Hell, S. W. Subdiffraction resolution in far-field fluorescence microscopy. *Optics Letters*. **24** (14), 954-956 (1999).
- Hell, S. W., Wichmann, J. Breaking the diffraction resolution limit by stimulated emission: stimulated-emission-depletion fluorescence microscopy. *Optics Letters*. **19** (11), 780-782 (1994).
- Gustafsson, M. G. L. Surpassing the lateral resolution limit by a factor of two using structured illumination microscopy. *Journal of Microscopy*. **198** (2), 82-87 (2000).
- Gustafsson, M. G. L. *et al.* Three-dimensional resolution doubling in wide-field fluorescence microscopy by structured illumination. *Biophysical Journal*. **94** (12), 4957-4970 (2008).
- Schermelleh, L. *et al.* Subdiffraction multicolor imaging of the nuclear periphery with 3D structured illumination microscopy. *Science*. **320** (5881), 1332-1336 (2008).
- Rust, M. J., Bates, M., Zhuang, X. Sub-diffraction-limit imaging by stochastic optical reconstruction microscopy (STORM). *Nature Methods*. **3** (10), 793-795 (2006).
- Betzig, E. *et al.* Imaging intracellular fluorescent proteins at nanometer resolution. *Science*. **313** (5793), 1642-1645 (2006).
- Balzarotti, F. *et al.* Nanometer resolution imaging and tracking of fluorescent molecules with minimal photon fluxes. *Science*. **355** (6325), 606-612 (2017).
- Vaughan, J. C., Jia, S., Zhuang, X. Ultrabright photoactivatable fluorophores created by reductive caging. *Nature Methods*. **9** (12), 1181-1184 (2012).
- Ha, T. *et al.* Probing the interaction between two single molecules: fluorescence resonance energy transfer between a single donor and a single acceptor. *Proceedings of the National Academy of Sciences of the United States of America*. **93** (13), 6264-6268 (1996).
- Roy, R., Hohng, S., Ha, T. A practical guide to single-molecule FRET. *Nature Methods*. **5** (6), 507-516 (2008).
- Huang, B., Wang, W., Bates, M., Zhuang, X. Three-dimensional super-resolution imaging by stochastic optical reconstruction microscopy. *Science*. **319** (5864), 810-813 (2008).
- Hua, B. *et al.* An improved surface passivation method for single-molecule studies. *Nature Methods*. **11** (12), 1233-1236 (2014).
- Fei, J. *et al.* RNA biochemistry. Determination of in vivo target search kinetics of regulatory noncoding RNA. *Science*. **347** (6228), 1371-1374 (2015).
- Raj, A., van den Bogaard, P., Rifkin, S. A., van Oudenaarden, A., Tyagi, S. Imaging individual mRNA molecules using multiple singly labeled probes. *Nature Methods*. **5** (10), 877-879 (2008).
- Stracy, M., Kapanidis, A. N. Single-molecule and super-resolution imaging of transcription in living bacteria. *Methods*. **120**, 103-114 (2017).
- Wang, S., Moffitt, J. R., Dempsey, G. T., Xie, X. S., Zhuang, X. Characterization and development of photoactivatable fluorescent proteins for single-molecule-based superresolution imaging. *Proceedings of the National Academy of Sciences of the United States of America*. **111** (23), 8452-8457 (2014).
- Sekar, R. B., Periasamy, A. Fluorescence resonance energy transfer (FRET) microscopy imaging of live cell protein localizations. *The Journal of Cell Biology*. **160** (5), 629-633 (2003).

21. Shi, X. *et al.* Super-resolution microscopy reveals that disruption of ciliary transition-zone architecture causes Joubert syndrome. *Nature Cell Biology*. **19** (10), 1178-1188 (2017).
22. Youn, Y., Ishitsuka, Y., Jin, C., Selvin, P. R. Thermal nanoimprint lithography for drift correction in super-resolution fluorescence microscopy. *Optics Express*. **26** (2), 1670-1680 (2018).